International Journal of Grid and Distributed Computing
Vol. 13, No. 1, (2020), pp. 851-859

Mitigation of SSR in Power System through Power Control of Additional DFIG

Dr. Nilaykumar A. Patel*[1], Mihir R. Patel[2]

[1,2] *Assistant Professor, Dept. of Electrical Engineering, CSPIT-CHARUSAT UNIVERSITY, Changa, Gujarat, India*

Abstract

This paper presents a direct power control strategy and its effect on sub-synchronous resonance (SSR) for doubly fed induction generator (DFIG) - based wind generator. When the synchronous generator undergoes a SSR, it will exchange power with series capacitor of transmission line. DFIG has power convertors in its rotor circuit, with the help of fast switching of IGBTs of rotor convertor circuit, fast control on active and reactive power of DFIG can be possible. The main objective of this paper is to examine the capability of DFIG to give active power and reactive power during SSR as per need. Apart from original test system, additional DFIG is included in test system and during sub-synchronous resonance its performance is analyzed without and with supplementary control signal from the synchronous generator. The analysis of SSR has been carried out based on transient simulation using MATLAB Simulink and eigenvalue analysis using D-Q model test system. The DFIG rotor convertor control to damp multimodal SSR oscillations comprises independent model control. The test system created from the system adopted from IEEE first benchmark model.

Keywords: *Sub-synchronous resonance, DFIG, IEEE First Benchmark Model, Eigenvalue Analysis, Rotor side convertor control.*

1. Introduction

Rapid exponentially increasing growth of electrical power demand forces the utilities to introduce the series capacitors in limited available transmission lines to overcome the effect of line reactance. However, this series capacitors will play a vital role to trigger sub synchronous oscillation in mass-spring system of turbine and generators due to negative damping [1], [2]. Due to transient disturbances magnification of shaft torque may be observed. This type of incident was reported in Mohave power plant in US, where two back to back successive shaft failure due to torsional SSR oscillations occurred in 1970 and 1971 [3], [4]. To prevent such type of incidents, different remedies like use of FACTS devices SSSC [5], SVC [6] and TCSC [7], control of excitation voltage [8], power system stabilizer with some modification [9] and inter plant power-flow controller [10] have been proposed. Fuzzy logic control for SVC to mitigate SSR has been proposed in [11]. Many of the suggested schemes can succeed to mitigate one oscillation mode but fail to supress other oscillation mode arise due to different level of series compensation. Hence, direction of thinking must be focus on a suitable source that can give required amount of power as per requirements. Many literatures give idea of direct power control of DFIG, which gives very good transient response. Here IEEE first benchmark modal (IEEE FBM) is used as test system with one modification. Apart from the test system given in IEEE FBM, one additional DFIG is introduced to support the mitigation of SSR in test system. Fast control capabilities of power convertor make DFIG most suitable to give required amount of power. Referring to the various literatures, the dominant strategy employed is a stator flux oriented vector control. [12]- [14]. The performance of the system affected by variation of actual system parameters with their actual value. The direct power control strategy without using rotor current [15] gives robust response even under the variation of parameters. The objective of the work is to test the role of new direct active and reactive power control strategy used for DFIG to supress the sub-synchronous oscillations. One input signal given to DFIG control circuit, which was derived from synchronous generator load angle.

The article is organized as follows: Test system is described in section II. Mathematical model of DFIG under D-Q frame is given in section III. Section IV gives the modelling of IEEE FBM test

ISSN: 2005-4262 IJGDC
Copyright ⓒ 2020 SERSC

system for SSR. Power control scheme of DFIG is covered in section V. Section VI consists of result and discussion and section VII draws conclusion.

2. Test System

The single line diagram of test system is illustrated in figure 1. In the said figure the test system is as per IEEE first benchmark model to study SSR except the DFIG. In the test system DFIG has total three masses but we are going to control the power of the DFIG, hence is considered as single mass model. DFIG will only participate in network mode due to its modelling strategy. Here chances of resonance become the same as the original IEEE First benchmark system. The generator may be considered as group of generators with same mechanical configuration. DFIG shown in the figure 1 may be from nearby wind generating station or it must be newly installed near to original generating station. The loading of the system is chosen such a way that the transformer doesn't get overloaded.

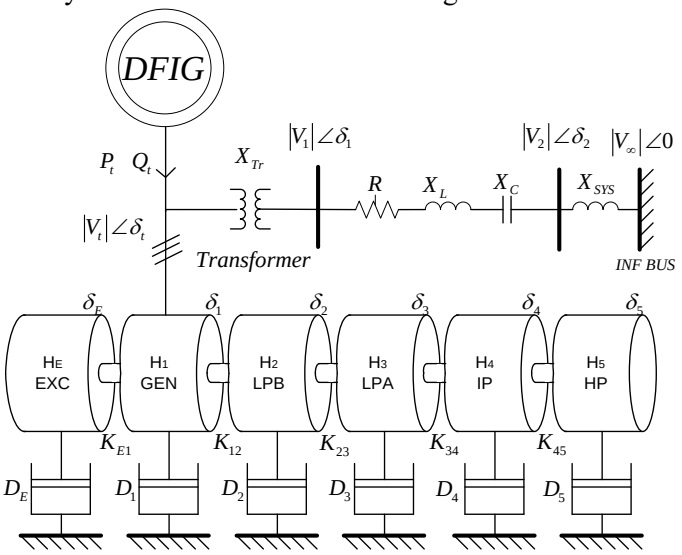

Figure 1. Adopted System for SSR Study with Rotor Configuration

To test the capabilities of DFIG, it is connected to a busbar of the synchronous generator. As per figure 2, the DFIG has rotor side convertors and the grid side convertors. The controlled power is fed to the transformer and hence finally to the grid. During the SSR oscillations, the control of DFIG rotor convertors are such that the mechanical mass system of synchronous generator will not remain in resonance with the series capacitor of transmission line.

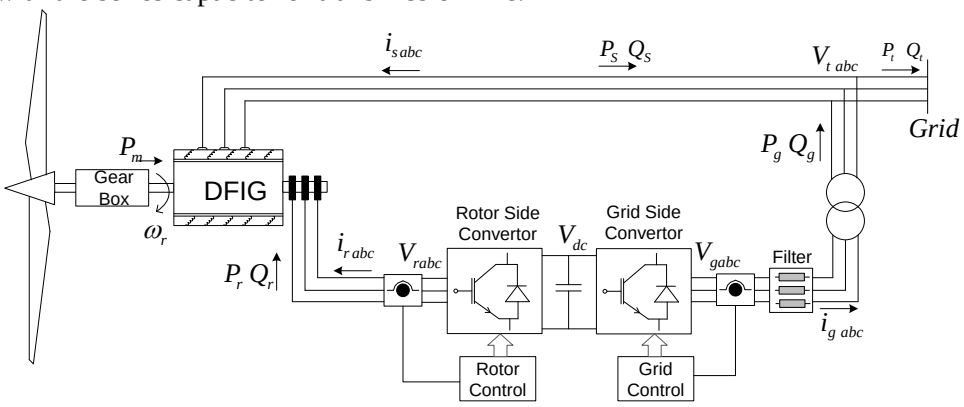

Figure 2. DFIG Based Wind Energy Conservation System

3. Modelling of DFIG for SSR Control

ISSN: 2005-4262 IJGDC
Copyright ⓒ 2020 SERSC

The DFIG is a wound rotor induction generator in which the rotor circuit is connected to grid with the back-to-back convertors, and the DC link is there between the convertors which is supported by capacitor bank. The fact acting IGBTs enables the fast output power control through rotor circuit in both directions. Hence either operating DFIG in sub-synchronous or Super-synchronous speed, control on SSR can be achieved. The well-known voltage and flux equations in the arbitrary reference frame and in D-Q form for DFIG are,

$$\left.\begin{aligned} v_{ds} &= R_s i_{ds} + p\psi_{ds} - \omega\psi_{qs} \\ v_{qs} &= R_s i_{qs} + p\psi_{qs} + \omega\psi_{ds} \end{aligned}\right\} \quad (1)$$

$$\left.\begin{aligned} v_{dr} &= R_s i_{dr} + p\psi_{dr} - (\omega - \omega_r)\psi_{qr} \\ v_{qr} &= R_s i_{qr} + p\psi_{qr} + (\omega - \omega_r)\psi_{dr} \end{aligned}\right\} \quad (2)$$

$$\left.\begin{aligned} \psi_{ds} &= L_s i_{ds} + L_m i_{dr} \\ \psi_{qs} &= L_s i_{qs} + L_m i_{qr} \end{aligned}\right\} \quad (3)$$

$$\left.\begin{aligned} \psi_{dr} &= L_m i_{ds} + L_r i_{dr} \\ \psi_{qr} &= L_m i_{qs} + L_r i_{qr} \end{aligned}\right\} \quad (4)$$

where $I_{ds}, I_{qs}, I_{dr}, I_{qr}$ are the currents of stator and rotor circuit, $\psi_{ds}, \psi_{qs}, \psi_{dr}, \psi_{qr}$ are flux linkages, ω_r is DFIG the rotor speed and R_s, R_r are the stator and rotor winding resistances respectively.

Under the synchronous reference frame, the above equations in matrix form will be as under,

$$\begin{bmatrix} v_{ds}^e \\ v_{qs}^e \end{bmatrix} = \begin{bmatrix} L_s p & -\omega_s L_s \\ \omega_s L_s & L_s p \end{bmatrix} \begin{bmatrix} i_{ds}^e \\ i_{qs}^e \end{bmatrix} + L_m \begin{bmatrix} p & -\omega_s \\ \omega_s & p \end{bmatrix} \begin{bmatrix} i_{dr}^e \\ i_{qr}^e \end{bmatrix} \quad (5)$$

$$\begin{bmatrix} v_{dr}^e \\ v_{qr}^e \end{bmatrix} = \begin{bmatrix} R_r + L_r p & -s\omega_s L_r \\ s\omega_s L_r & R_r + L_s p \end{bmatrix} \begin{bmatrix} i_{dr}^e \\ i_{qr}^e \end{bmatrix} + L_m \begin{bmatrix} p & -s\omega_s \\ s\omega_s & p \end{bmatrix} \begin{bmatrix} i_{ds}^e \\ i_{qs}^e \end{bmatrix} \quad (6)$$

where s is the slip and *e* denotes synchronous reference frame. Now from equation (5),

$$\begin{bmatrix} i_{ds}^e \\ i_{qs}^e \end{bmatrix} = \frac{1}{L_s\left(p^2 + \omega_s^2\right)} \begin{bmatrix} p & \omega_s \\ -\omega_s & p \end{bmatrix} \left\{ \begin{bmatrix} v_{ds}^e \\ v_{qs}^e \end{bmatrix} - L_m \begin{bmatrix} p & -\omega_s \\ \omega_s & p \end{bmatrix} \begin{bmatrix} i_{dr}^e \\ i_{qr}^e \end{bmatrix} \right\} \quad (7)$$

Subsisting equation (7) into (6), and eliminate i_{ds}^e and i_{qs}^e, and transient equation of the rotor voltages in synchronous reference frame for the DFIG received as under,

$$\begin{bmatrix} v_{dr}^e \\ v_{qr}^e \end{bmatrix} = \begin{bmatrix} R_r + L_r' p & -s\omega_s L_r' \\ s\omega_s L_r' & R_r + L_r' p \end{bmatrix} \begin{bmatrix} i_{dr}^e \\ i_{qr}^e \end{bmatrix} + D \cdot \begin{bmatrix} v_{ds}^e \\ v_{qs}^e \end{bmatrix} \quad (8)$$

where L_r' is the rotor transient inductance, $L_r' = \sigma L_r$ where $\sigma = 1 - L_m^2 / (l_s L_r)$ and

$$D = \frac{L_m}{L_s} \frac{1}{p^2 + \omega_s^2} \begin{bmatrix} p^2 + s\omega_s^2 & (1-s)\omega_s p \\ (s-1)\omega_s p & p^2 + s\omega_s^2 \end{bmatrix} \quad (9)$$

The DFIG active and reactive powers are computed as under,

$$P_s = \frac{3}{2}\left(v_{ds} i_{ds} + v_{qs} i_{qs}\right) = -\frac{3}{2}\frac{L_m}{L_s} v_{qs} i_{qr} \quad (10)$$

$$Q_s = \frac{3}{2}\left(v_{qs} i_{ds} - v_{ds} i_{qs}\right) = \frac{3}{2} v_{qs}\left(\frac{L_m}{L_s} i_{dr} - \frac{v_{qs}}{\omega_s L_s}\right) \quad (11)$$

The terminal voltage can be kept constant by placing SVC type device and hence, the stator active and reactive power can be controlled by means of rotor currents.

ISSN: 2005-4262 IJGDC
Copyright ⓒ 2020 SERSC

4. Modeling of Rest of the System

The state-space equations derived from D-Q modelling of the test system is adopted here [16]. To carryout eigenvalue analysis, linearized equations around operating point are derived. The linearized equations of turbine-generator and transmission line with series capacitor are derived and state-space matrix constructed. Rotor model of generator is shown in figure 1.

4.1. Modeling of Synchronous Machine

Synchronous machine model of type 2.2 is used for the synchronous generator. Stator consists of three phase winding and the rotor has one field winding and one damper winding on D axis and two damper windings on Q axis. Detailed modelling is done in this analysis to capture accurate dynamics of rotor. The space-state equations of each generator can be derived from the following basic equations.

$$\psi_S = [L_{ss}]i_s + [L_{sr}]i_r \quad (12)$$

$$\psi_r = [L_{rs}]i_s + [L_{rr}]i_r \quad (13)$$

The matrices in above equations are of stator and rotor self and mutual inductance. The above equations are converted in D-Q form and then linearized.

4.2. Modeling of Multi-Mass Turbine-Generator Set

The turbine-generator mechanical system shown in Figure 1 is represented by one stage of generator mass, one stage of exciter and four stages of turbine masses. These six masses of turbo generator are of different inertias are interconnected by five soft steel shafts and can be represented by following shaft torque equations given in (14).

$$[2H]p^2\underline{\delta} + [D]p\underline{\delta} + [K]\underline{\delta} + \underline{T} = 0 \quad (14)$$

Where [D] and [H] are diagonal matrix of damping and inertia coefficients, respectively, and shaft stiffness matrix is denoted by [K]. T gives torque vector acting on the shaft end and δ is the resulting angular position vector. The inertia constants, damping coefficient and shaft stiffness of different stages are given in Appendix A. In this paper damping is ignored. The state variable considered is the speed and angular displacement of each mass.

From the equation (14), the state matrix A can be obtain for both of the generators and the solution of A matrix gives the eigenvalues, from the eigenvalues natural frequencies of multi mass model are calculated, which are listed in table 1.

Table 1. Modes and Corresponding Frequency

Mode	Natural frequency (Hz)
Mode 0	1.67
Mode 1	15.71
Mode 2	20.21
Mode 3	25.55
Mode 4	32.3
Mode 5	47.3

4.3. Modeling of Electric Network

The electrical equivalent circuit for the IEEE first benchmark model to study SSR is shown in Fig. 3. The generator with constant voltage source Eg and with terminal voltage of Vt is connected to infinite bus through series compensated transmission line. The state equations of electrical network in d–q components are given in (15) and (16).

ISSN: 2005-4262 IJGDC
Copyright ⓒ 2020 SERSC

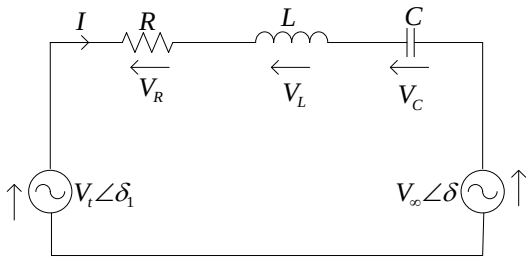

Figure 3. Electric Network Model of Test System

$$\left.\begin{aligned} V_{td} &= Ri_d + \frac{X_L}{\omega_0} pi_d - \frac{\omega}{\omega_0} X_L i_q + v_{cd} + V_\infty \sin\delta \\ V_{tq} &= Ri_q + \frac{X_L}{\omega_0} pi_q + \frac{\omega}{\omega_0} X_L i_d + v_{cq} + V_\infty \cos\delta \end{aligned}\right\} \quad (15)$$

$$\left.\begin{aligned} pv_{cd} &= \omega v_{cq} + \omega_0 X_C i_d \\ pv_{cq} &= -\omega v_{cd} + \omega_0 X_C i_q \end{aligned}\right\} \quad (16)$$

5. Power Control Scheme of DFIG

In the proposed control strategy, the D-axis of the synchronous frame is fixed to the stator flux. The stator is directly connected to the grid, hence the effect of the stator resistance can be neglected, and the stator flux can be held constant. From equation (1), for a synchronous frame, the stator voltage vector is given as,

$$v_{qs} = \omega_s \psi_{ds} \quad (17)$$

Since the power coefficient for wind turbine is always maintained at its optimal value, using equations (10) and (11), the stator active and reactive power can be computed as,

$$\left.\begin{aligned} P_s &= -k_\sigma \omega_s \psi_{ds}^{\omega} \psi_{qr}^{\omega} \\ Q_s &= k_\sigma \omega_s \psi_{ds}^{\omega} \left(\frac{L_r}{L_m} \psi_{ds}^{\omega} - \psi_{dr}^{\omega} \right) \end{aligned}\right\} \quad (18)$$

where $k_\sigma = 1.5L_m / (\sigma L_s L_r)$

As the stator flux remains constant, according to above set of equation the required change in active and reactive power to control oscillations of synchronous generator over a small period of time is given by,

$$\left.\begin{aligned} \Delta P_s &= -k_\sigma \omega_s \psi_{ds}^{\omega} \Delta\psi_{qr}^{\omega} \\ \Delta Q_s &= -k_\sigma \omega_s \psi_{ds}^{\omega} \Delta\psi_{dr}^{\omega} \end{aligned}\right\} \quad (19)$$

Combining equations (8), (18) and (19) and neglecting the rotor resistance, we are getting the rotor voltage required to control power, which is as under,

ISSN: 2005-4262 IJGDC
Copyright ⓒ 2020 SERSC

$$\left.\begin{aligned} v_{dr}^{\omega} &= \left(K_{P_Q} + \frac{K_{I_Q}}{s}\right)\left(Q_s - Q_s^*\right) + \omega_{sl}\frac{P_s}{k_\sigma \omega_s \psi_{ds}^{\omega}} \\ v_{qr}^{\omega} &= \left(K_{P_p} + \frac{K_{I_p}}{s}\right)\left(P_s - P_s^*\right) + \omega_{sl}\left(\frac{L_r}{L_S}\psi_{ds}^{\omega} - \frac{Q_s}{k_\sigma \omega_s \psi_{ds}^{\omega}}\right) \end{aligned}\right\} \quad (20)$$

The schematic control diagram is shown in figure 4, in which ΔP_G signal is derived from the synchronous generator. The power exchange done by synchronous generator during sub-synchronous resonance will be compensated by DFIG by ΔP_G signal. This signal will become active only during sub-synchronous resonance.

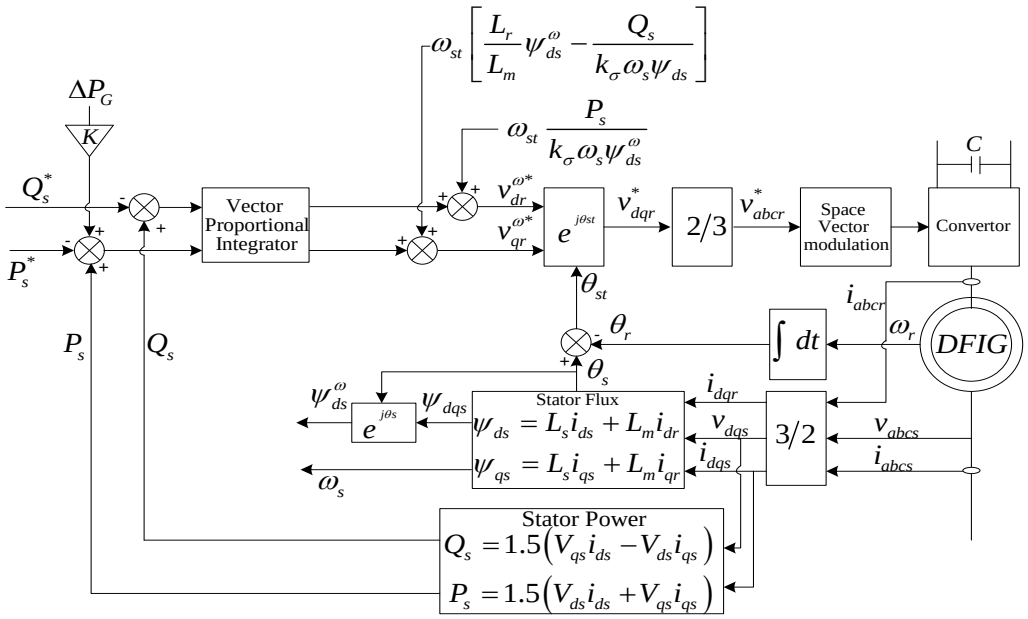

Figure 4. Schematic diagram of the proposed control scheme for DFIG

6. Result and Discussion

In this paper, three different cases with different level of compensation has been examined.

Case I: The overall base system without DFIG.

Case II: Test system with DFIG but without control signal from synchronous generator.

Case III: Test system with DFIG with control signal from synchronous generator.

For all the cases, two sub cases with the series compensation level of 50% and 25% are tested. The reason behind using this particular level of compensation is to excite different torsional mode of synchronous generator. The objectives of the work are to carry out eigenvalue analysis for all above listed cases and to investigate the effect of DFIG power control strategy with series compensation on SSR. The eigenvalue analyses for first case has been reported in Table 2 to identify the torsional modes which have the frequency of oscillations in sub-synchronous frequency range.

Some torsional modes are highlighted which have the positive real part which is responsible to create sub-synchronous resonance in the system. The use of DFIG with transient active power control strategy can improve one of the torsional modes as compared to base system but not fully succeed to mitigate SSR. The addition of power control strategy of DFIG can improve the torsional mode but left the system with insufficient damping.

In order to mitigate the impact of SSR and to stabilize the system with series compensation, the application of derived control signal from synchronous generator has been explored. It can be noticed from Table 3 that the use of generator power deviation as a supplementary signal can successfully

ISSN: 2005-4262 IJGDC

Copyright ⓒ 2020 SERSC

mitigating all torsional modes and make the system stable. All eigenvalues shows the negative real parts and results in higher damping even with 50% or 25% of compensation level.

Table 2. Result of Eigenvalue analysis for Case I

Test system with 50% series compensation without DFIG	Test system with 25% series compensation without DFIG	Modes of Oscillations
± 297.97i	-0.08± 293.97i	Torsional mechanical mode of synchronous generator
-0.009 ± 202.804i	-0.162 ± 205.79i	
-0.016 ± 160.41i	-0.15 ± 162.34i	
0.143 ± 126.798i	**0.186 ± 127.01i**	
0.405 ± 99.030i	-0.05 ± 98.85i	

Table 3. Result of Eigenvalue analysis for Case II and Case III

Test system with DFIG but without control signal from synchronous generator		Test system with DFIG with control signal from synchronous generator		Modes of Oscillations
50% series compensation	25% series compensation	50% series compensation	25% series compensation	
-0.001± 298.74i	-0.012± 290.97i	-0.014± 295.47i	-0.02± 295.05i	Torsional mechanical mode of synchronous generator
-0.009 ± 201.51i	-0.412 ± 204.27i	-0.045 ± 201.87i	-0.062 ± 202.02i	
-0.021 ± 160.02i	-0.44 ± 163.7i	-0.078 ± 160.64i	-0.084 ± 160.62i	
-0.023 ± 126.21i	**0.09 ± 126.95i**	-0.049 ± 126.81i	-0.051 ± 127.59i	
0.124 ± 99.510i	-0.072 ± 98.02i	-0.045 ± 98.81i	-0.0532 ± 97.74i	

Time domain simulations are also carried out for case II and case III for 50% compensation level in MATLAB-Simulink using derived equations. Figure 5 and figure 6 shows the time domain response of oscillations of masses and the shaft torque between LPA and LPB turbine of generator 1for the disturbance applied at t = 10 seconds for case II and case III respectively. The results of time domain simulations validate the results obtained from the eigenvalue analysis.

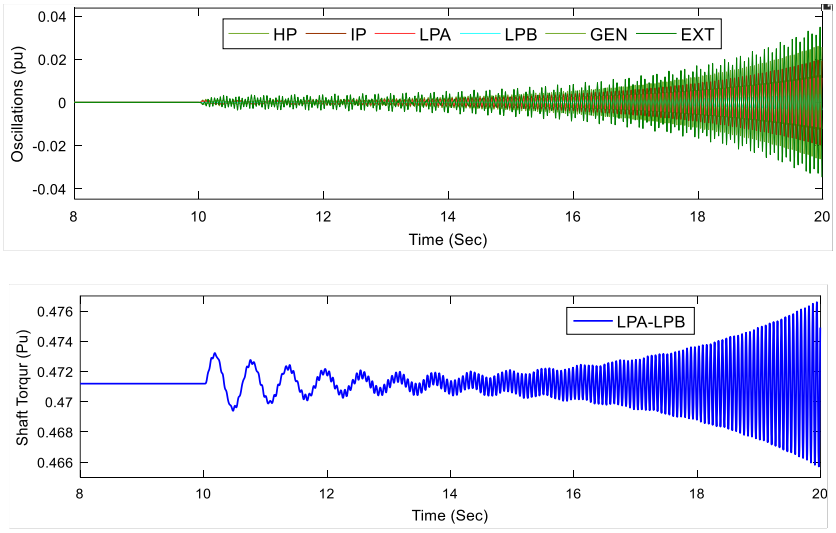

Figure 5. Oscillations of Masses and LPA-LPB Shaft Torque of Generator 1 for Case II

ISSN: 2005-4262 IJGDC
Copyright ⓒ 2020 SERSC

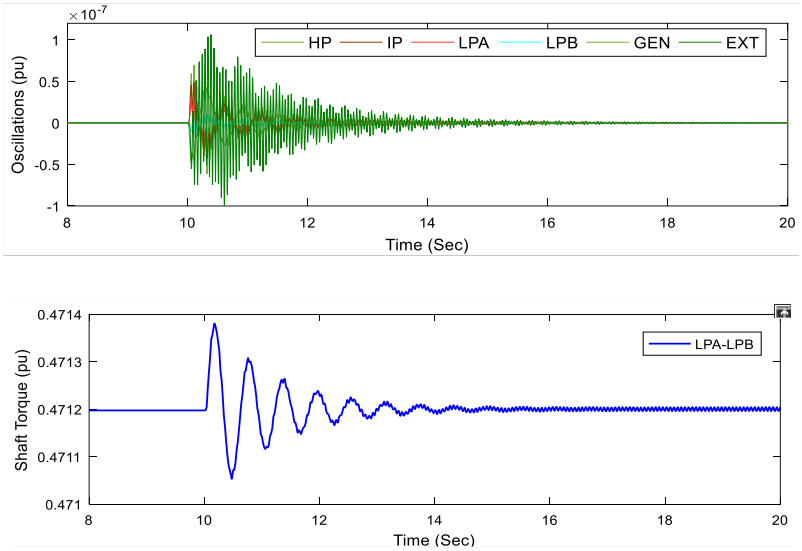

Figure 6. Oscillations of Masses and LPA-LPB Shaft Torque of Generator 1 for Case III

7. Conclusion

The paper presents the state space modelling of different electrical components to study impact of interplant power flow controller on SSR of the test system derived from IEEE FBM to study sub-synchronous resonance. The series compensation of transmission network with certain degree of compensation may result in SSR. With different component modelling, a systematic approach is presented with transient modelling of DFIG with active and reactive power control loop. Two different level of compensation, 25% and 50% are considered to excite modes from turbo generator. From eigenvalue analysis and time domain simulation, it is concluded that when DFIG is use with only its power control loop, it cannot succeed to damp all the torsional oscillations of the generator. When the DFIG is used with supplementary signal derived from the power oscillation of turbo generator, all the torsional modes can be damped even if the compensation level matches with the natural frequency of turbine-generator set.

Appendix

IEEE FBM values in pu.

X_T=0.14 pu, R_L=0.02, X_L=0.50, X_{SYS}=0.06, X_C=0.371, P_g=0.9, V_T=1

Mechanical masses value Generator 1

Inertia	Inertia Constant (H)	Shaft section	Spring Constant (K) in pu torque/rad
HP turbine	0.092897	HP-IP	19.303
IP turbine	0.155589	IP-LPA	34.929
LPA turbine	0.85867	LPA-LPB	52.038
LPB turbine	0.884215	LPB-GEN	70.858
Generator	0.868495	GEN-EXC	2.82
Exciter	0.034217		

References

[1] IEEE Committee Report, "Readers Guide to subsynchronous resonance", IEEE Trans. Power System, vol. 7, no. 1, (1992), pp. 150-157.
[2] Kundur P. Power System Stability and Control, New Delhi: McGraw Hill, (2012).

ISSN: 2005-4262 IJGDC
Copyright ⓒ 2020 SERSC

[3] P.M. Anderson, B.L. Agrawal and J.E. Van Ness, Subsynchronous resonance in power systems (1st ed.). New Jersey: Wiley-IEEE Press. (1999).
[4] IEEE SSR Working Group, "Countermeasures to subsynchronous resonance problems", IEEE Transactions on Power Apparatus and Systems, vol. PAS-99, no. 5, (1980), pp. 1810-1818.
[5] N. A. Patel and P. Bhatt, "SSR Mitigation in Power System with Static Synchronous Series Compensator", International Journal of Engineering and Technology. vol. 7, no. 3, (2018) pp. 1457-1462.
[6] N. A. Patel and P. Bhatt, "Mitigation of Sub-Synchronous Resonance with Static Var Compensator", Journal of Engineering Science and Technology, vol. 14, no. 2, (2019), pp. 1101-1117.
[7] Z. Rui, Li Gen and J. Liang, "Capability of TCSC on SSR Mitigation", Journal of Power and Energy Engineering, vol. 03, (2015), pp. 232-239.
[8] X. Xie, H. Liu and Y. Han, "Coordinated Design of Supplementary Excitation Damping Controller and Voltage-sourced Converter Based Generator Terminal Subsynchronous Damping Controller for Subsynchronous Resonance Suppression: A Case Study", Electrical Power Components and System, vol. 44, no. 5, (2016), pp. 565-577.
[9] M. R. Patel and N. A. Patel, "Enhancement of Transient Stability on Power System with The Use of Power System Stabilizer", 2016 International Conference on Electrical, Electronics, and Optimization Techniques (ICEEOT), Chennai, India, (2016), March 3-5.
[10] N. A. Patel and M. R. Patel, "Analysis of SSR with Interplant Power-Flow Controller", Journal of Xidian University, Vol. 14, no. 4, (2020), pp. 15-22.
[11] S.T. Nagarajan and N. Kumar, "Fuzzy logic control of SVS for damping SSR in series compensated power system". International Transactions on Electrical Energy Systems, vol. 25, no. 9, (2015), pp. 1860-1874.
[12] K. Kerrouche, A. Mezouar, and Kh. Belgacem, "Decoupled Control of Doubly Fed Induction Generator by Vector Control for Wind Energy Conversion System," Energy Procedia, vol.42, (2013), pp. 239-248.
[13] R. Cárdenas, R. Peña, S. Alepuz, and G. Asher, "Overview of control systems for the operation of DFIGs in wind energy applications," IEEE Transactions on Industrial Electronics, vol. 60, no. 7, (2013), pp. 2776–2798.
[14] G. D. Marques, and D. M. Sousa, "New sensorless rotor position estimator of a DFIG based on torque calculations-stability study," IEEE Transactions on energy Conversion, vol. 27, no.1, (2012), pp. 196–203.
[15] R. Datta and V. Ranganathan, "Direct Power Control of Grid-Connected wound rotor Induction Machine without Rotor Position Sensors". IEEE Transactions on Power Electronics, vol. 16, no. 3, (2001), pp. 390-399.
[16] P.C. Krause, O. Wasynczuk and S.D. Sudhoff, "Analysis of electric machinery and drive systems (2nd ed.). New Jersey: Wiley-IEEE Press. (2002).

ISSN: 2005-4262 IJGDC
Copyright ⓒ 2020 SERSC